Journal Of Animal Ecology
October 2021, Volume 90 Issue 10 Pages 2302-2314
https://doi.org/10.1111/1365-2656.13536
https://archimer.ifremer.fr/doc/00699/81095/

Sharks surf the slope: Current updrafts reduce energy expenditure for aggregating marine predators

Papastamatiou Yannis P. [1, *] , Iosilevskii Gil [2], Di Santo Valentina [3], Huveneers Charlie [4], Hattab Tarek [5], Planes Serge [6, 7], Ballesta Laurent [8], Mourier Johann [9]

[1] Institute of the Environment Department of Biological Sciences Florida International University North Miami FL ,USA
[2] Faculty of Aerospace Engineering Technion Haifa ,Israel
[3] Division of Functional Morphology Department of Zoology Stockholm University Stockholm ,Sweden
[4] College of Science and Engineering Flinders University Bedford Park South Australia ,Australia
[5] MARBEC, Univ Montpellier CNRS IFREMER IRD Sète, France
[6] PSL Research University EPHE-UPVD-CNRS USR 3278 CRIOBE Perpignan ,France
[7] Laboratoire d'Excellence “CORAIL” USR 3278 CNRS-EPHE-UPVD CRIOBE Perpignan ,France
[8] Andromede Oceanology Carnon ,France
[9] MARBEC, Univ Montpellier CNRS IFREMER IRD Sète, France

* Corresponding author : Yannis P. Papastamatiou, email address : ypapastamatiou@gmail.com

Abstract :

1. An animal's energy landscape considers the power requirements associated with residing in or moving through habitats. Within marine environments, these landscapes can be dynamic as water currents will influence animal power requirements and can change rapidly over diel and tidal cycles.

2. In channels and along slopes with strong currents, updraft zones may reduce energy expenditure of negatively buoyant fishes that are also obligate swimmers. Despite marine predators often residing within high-current area, no study has investigated the potential role of the energetic landscape in driving such habitat selectivity.

3. Over 500 grey reef sharks Carcharhinus amblyrhynchos reside in the southern channel of Fakarava Atoll, French Polynesia. We used diver observations, acoustic telemetry and biologging to show that sharks use regions of predicted updrafts and switch their core area of space use based on tidal state (incoming versus outgoing).

4. During incoming tides, sharks form tight groups and display shuttling behaviour (moving to the front of the group and letting the current move them to the back) to maintain themselves in these potential updraft zones. During outgoing tides, group dispersion increases, swimming depths decrease and shuttling behaviours cease. These changes are likely due to shifts in the nature and location of the updraft zones, as well as turbulence during outgoing tides. Using a biomechanical model, we estimate that routine metabolic rates for sharks may be reduced by 10%–15% when in updraft zones.

5. Grey reef sharks save energy using predicted updraft zones in channels and ‘surfing the slope’. Analogous to birds using wind-driven updraft zones, negatively buoyant marine animals may use current-induced updraft zones to reduce energy expenditure. Updrafts should be incorporated into dynamic energy landscapes and may partially explain the distribution, behaviour and potentially abundance of marine predators.

Keywords : biologging, energy seascape, grey reef sharks, tides

Introduction

Animal locomotory costs will partially depend on the habitats they move through or reside in, and will contribute to their overall fitness and energy surplus. The spatial representation of animal's cost of transport (COT, energy spent to move a unit distance) is termed the energy landscape, and may explain animal behavior, distribution patterns, movement paths, and foraging ranges (Furness and Bryant 1996, Wall et al. 2006, Wilson et al. 1991, 2012, Shepard et al. 2013). Furthermore, while energy landscapes can explain habitat selection at the local level, these effects may scale up and provide an understanding of global patterns of distribution or even animal migrations (e.g. Amélineau et al. 2018, Somveille et al. 2018). Terrestrial animals face largely static energy landscapes as the COT will depend on factors such as ground substrate (e.g. sand vs rock) and slope (Wall et al. 2006, Dunford et al. 2020), but will remain relatively consistent through time (although rain and snow may cause some changes, Wilson et al. 1991). However, animals in fluid environments face much more dynamic landscapes, as water and air currents can change over annual, seasonal and hourly time frames, and animals have the option to select vertical habitats in addition to horizontal ones (Shepard et al. 2013). For example, the energy costs of flying seabirds will vary with wind speeds and direction which can change over a range of temporal and spatial scales (Furness and Bryant 1996, Amélineau et al. 2014).

Within terrestrial environments, updrafts (vertical currents) may form due to uneven heating (thermal updrafts) or from horizontal winds deflecting off slopes and mountain ranges (orographic updrafts, Shepard et al. 2013, Duerr et al. 2019, Scacco et al. 2019). Updrafts will contribute to the energy landscape of birds, as they can counteract the effects of gravity by generating lift beneath the extended wings (e.g. Duerr et al. 2019). Field measurements of activity have identified updraft zones as regions where some birds can greatly reduce their energy costs while flying (Amélineau

et al. 2014, Scacco et al. 2019). Subsequently, many bird species will select regions where updrafts occur and some species may actually require them to meet the energy demands of flight (Weimerskirch et al. 2016, Williams et al. 2020).

While the influence of dynamic energy landscapes on bird movements are well established, far less is known for animals in marine environments. Within marine environments, water currents will also contribute to the energy seascapes of fishes and will be highly dynamic as currents can change in strength, direction, and location over short time periods. Tides may cause changes in current direction and strength several times per day, and potentially even flow dynamics (e.g. laminar vs turbulent flow). Fishes living in areas with strong currents may swim with the current, likely as a mechanism to conserve energy (Brill et al. 1993, McInturf et al. 2019) or select regions where currents are weaker (e.g. in the lee of rocks or underwater structures, Liao 2007). Sturgeon (*Scaphirhynchus albus*) will swim along the edges of river-banks where currents are weakest, presumably as their COT is reduced in these regions (McElory et al. 2012). Currents striking slopes in bottom topography should also generate orographic updrafts similar to those from winds in terrestrial environments (O'Dor et al. 2002). These updrafts may provide an energetic refuge for negatively buoyant animals that rely on body surfaces to generate hydrodynamic lift (e.g. pectoral fins of sharks, Harris 1936, Lauder and Di Santo 2015). Sharks are negatively buoyant and generate hydrodynamic lift via their forward motion but will have a minimal stalling speed below which they will start to sink (Harris 1936, Di Santo et al. 2017). Many species of shark are obligate ram ventilators and must swim continuously to extract enough oxygen across the gills to meet metabolic demands. As there is no difference in physical mechanisms underlying flying and swimming of negatively buoyant animals, swimming in updrafts should reduce the sharks swimming effort and subsequent energetic costs. Obligate swimming sharks have been observed

hovering in high current regions, although the mechanisms behind this behavior were not explored (Wheeler et al. 2013). Negatively buoyant squid also appear to use slope regions where updrafts may exist, although the energy savings of 'surfing the slope' were not quantified (O'Dor et al. 2002). It is therefore possible that sharks may exploit updrafts to reduce the postural and hydrodynamic costs of swimming.

The southern channel at Fakarava Atoll, French Polynesia, experiences strong tidally-induced currents, and up to 500 grey reef sharks (*Carcharhinus amblyrhincos*) reside there (Mourier et al. 2016). These sharks are highly active (hunting) at night, but cruise slowly during the day (Mourier et al. 2016, Labourgade et al. 2020). We hypothesize that during the day sharks are using updraft zones originating from rising slopes in the channel, to reduce movement-induced energy costs. We predict that if sharks are using updrafts then a) they should use regions of the channel with a rising seafloor relative to incoming direction of tidal currents (likely location of updrafts), b) sharks should shift position between incoming vs outgoing tides as updraft locations will also move, c) sharks will face into the current but when they move out of updraft zones they will use the current to move them back into the zone and exhibit shuttling behavior, d) relative energy expenditure of sharks in the channel should be less than for sharks residing outside the channel.

Methods

Study site

This study was conducted at the southern channel of Fakarava atoll, in the Tuamotu archipelago of French Polynesia (16°30' S 145°27' W). The channel is only 1 km long, 200 m across, with maximum depths of approximately 30 m, and tidally flushed every 6 h (Fig. 1). There is a single entrance to the channel from the ocean but it splits into two smaller channels before

connecting to the lagoon. At the entrance to the channel is a steep drop off connecting to open ocean environments. Approximately 500 grey reef sharks reside within the channel, with highest levels of residency from May to October, which coincides with periods of grouper spawning (Mourier et al. 2016). Sharks form 2–3 groups within the channel, with two consistent groups inside the channel and a smaller one at the drop-off on the southern entrance (Mourier et al. 2016, Supplementary material A).

Within terrestrial environments, updrafts can be located based on topography and slope features (Duerr et al. 2019, Scacco et al. 2019). We had access to a high-resolution bathymetry map of the Fakarava channel, which was constructed from the multibeam sonar system (MBSS) GeoSwath (Mourier et al. 2016). During 2014, a boat equipped with a MBSS did a series of transects in the pass to measure depth and map the bathymetry at a resolution of 1 meter (Supplementary material A). Current direction runs South to North during incoming tides and North to South during outgoing tides. Consequently, we expect that the incoming tide will create updrafts in those segments of the channel where the bottom rises towards the North, whereas the outgoing tide will create updrafts in those segments of the channel where the bottom rises toward the South. We did not have access to direct measurements of current speeds, but based on the ability of a diver to swim against the current, and measured current speeds within the channels of Hao and Avatoru atolls (with similar characteristics to Fakarava, Rougerie and Gros 1980, Marigliano and Taquet 2011), we estimate them to be approximately 0.5 m/sec. We simulated the updrafts for a simplified geometry of the channel using in-house code that followed the paradigm of the discrete vortex method (Katz and Plotkin, 1991). The geometry was based on the true profile of the channel in the South-North direction, but assumed constant depth (and width) in the East-West direction. Spatial resolution in the South-North direction was 1 m.

Acoustic telemetry

We caught 38 grey reef sharks within the channel in June 2017. Sharks were caught at night or during the morning by divers. A diver would grasp the tail of a shark as it swam by and a line from a boat on the surface was secured to the shark's tail, and used to bring the shark to the surface, where it was restrained alongside the boat. The shark was then inverted on its back to induce tonic immobility (Mourier et al. 2016, Williamson et al. 2018, Papastamatiou et al. 2018a, b). We made an incision in the ventral surface of the shark and surgically implanted a V13AP acoustic transmitter (69 kHz, Innovasea, Nova Scotia), before closing the incision with surgical staples and releasing the animal. The transmitters were detected by a network of 25 underwater listening stations (VR2W, Innovasea, Nova Scotia) installed within the channel and one station northeast of the channel (Fig. 1A). Every time a shark swam within range of a listening station, the VR2W logged the date and time of detection, each transmitter's unique ID, as well as the animal's swimming depth (from pressure sensors on the transmitters) and its activity (acceleration). Range testing inside the channel showed detection ranges of approximately 100 m (50% detection probability) and 50 m (100% detection probability) during the day. Consequently, all receivers were spaced 50 m apart. Acceleration (range ± 4.9 m s^{-2}, resolution 0.02 m s^{-2}) and depth (accuracy ± 1 m, resolution 0.3 m) data were transmitted at random intervals between 100–160 s for the first 120 days, after which the random interval was 50–110 s. Acceleration was sampled at 5 Hz for 20 seconds, four times every five transmission cycles. Acceleration was calculated as an average root mean square absolute value for all three axes and transmitted as an 8-bit digital value. The static contribution to overall *g* was filtered out prior to root mean square calculation via manufacturer on-board algorithms. All receivers were downloaded a year later in June 2018. To avoid seasonal and diel changes in behavior, we only analyzed data from April to June 2018, and during daylight

hours. The remaining data was split into incoming and outgoing tidal periods. We removed the first and last hours of tidal stages to avoid any noise in behavior due to slack tide duration, and only included the well-established 4-h tidal stages.

We used the *adehabitatHR* package in R to calculate the kernel utilization distributions (KUD) for sharks within the channel. To do this, we 1) used the Center of Activity (COA) method (Simpfendorfer et al. 2002) to estimate the location of sharks over 10 minute intervals, and then 2) used the locations to calculate fixed KUDs based on the spatial distribution of positions. Core activity space is estimated by calculating the area within the 50% contour of KUDs, while the full extent of the activity space is estimated by calculating the area within the 95% contour. We could estimate the distance between tagged sharks every 10 minutes during tidal stages by calculating the distances in meters between individual COA positions. These are not a measure of nearest neighbor distances, but can be used as a measure of group dispersion. We compared swimming depths, activity and inter-individual distances between tidal states using generalized linear mixed models (GLMM), and included individual as a factor to account for repeated measures from the same individual. GLMMs were run using the *nlme* package in R.

To assess if sharks were selecting updraft zones, we compared the proportion of COA positions that occurred within predicted updraft zones (dependent on tidal state) to those of randomly walking sharks. Randomizations were used to generate points within the confines of the acoustic array (i.e. where they can be detected) using a Random Walk model for each shark, and the proportion of time spent in updraft zones were compared between empirical data and randomizations using a melted binomial test. Finally, we calculated occupational densities for all sharks to overlay with updraft models, using the COA positions (sampled every 10 min) and swimming depth sampled every 1 hour. The channel was divided into 20 x 20 m squares and the

density of space use was calculated based on the number of times sharks were found within squares. Swimming depths of the sharks were averaged over the time periods sharks were detected within a square. All statistical analyses were performed in R ver. 3.6.3.

Group kinematics

To determine how sharks behaved while in the group, we observed and filmed their swimming behavior within the channel in May–June 2017 and 2018. Filming dives were performed during daytime, incoming tides, using closed-circuit rebreathers (which produce no bubbles). Divers swam at an average depth of 25 m and wedged themselves between rocks to film the sharks from below, minimizing the chance of disturbing their behavior. We recorded shark behavior using Hero 3 and 4 GoPro at 30 fps. Videos were uploaded in GoPro Studio and selected sequences were saved as *avi* files to be analyzed in Photron Viewer Software v.353 (Photron, San Diego). For each sequence and group (total of 16 groups), we randomly selected 5 individuals in the front of the group (the south section) and 5 individuals in the mid/back section of the group (north section) and tail beat frequency (TBF Hz) was measured as one complete tail beat cycle divided by time (s). Data from these sequences were analyzed using a 2-way ANOVA, with group ID and position as factors. Additionally, we measured TBF in individuals that shifted their position from leading (front of the group) to trailing (where individuals swim behind other sharks), to account for inter-individual variation in TBF and position (n=10). Data on shifting position were analyzed using a 1-way ANOVA with position as a factor. Observations were only made from the shark groups inside the channel.

Biologging

To get fine-scale measurements of activity and swimming kinematics, we deployed CATS (Customized Animal Tracking Solutions, Germany) data-loggers on sharks we caught in the

channel. Tags were fitted to the dorsal fin with galvanic links, and then released. When the galvanic link dissolved, the package released from the animal and floated to the surface. Embedded VHF (Advanced Telemetry Systems Inc., MN, USA) and SPOT (Wildlife Computers Inc., WA, USA) satellite transmitters then enabled us to locate and recover the loggers. Sensors included 3D accelerometer, 3D rate-gyro, 3D magnetometer (all recording at 20 Hz), and depth and water temperature (1 Hz). The loggers also included a HD video camera with recording duration of 4–5 h. For one shark, the video failed to turn on, while for another the video worked but the diary failed to record. Two other animals tagged during the night, had the tags detach prematurely before the video could turn on. We discarded the first hour of data to avoid periods of high swimming activity associated with stress of capture. This time period was selected based on a return to baseline activity (acceleration) within one hour and based on camera tag footage which showed sharks returning to the group. We would also dive approximately one hour after releasing the shark and in all cases would see the tagged animal back within the group and behaving similarly to other sharks. A high pass filter was used to separate static and dynamic acceleration, and the product of the three axes were used to calculate overall dynamic body acceleration (ODBA) as a measure of activity. We used the tri-axial magnetometer to quantify the 'pseudo-heading' of the sharks using the dead reckoning methods described by Bidder et al. (2015). We did not use the magnetometer to produce an accurate track of the animal but rather to determine when (and how often) the animals were changing direction, relative to tidal state.

To determine the potential benefit of swimming in the channel, we compared swimming effort against the sink rate (rate of descent). Swimming effort was associated with the variance of the yaw rate (angular rate measured by the rate-gyro around the dorso-ventral axis). At a given swim speed, thrust should be proportional to the lateral velocity of the tail squared (Yates 1984);

for comparably sized sharks the yaw rate is a proxy for the lateral velocity. For each shark, we compared the proportionality factor between the variance of yaw rate and the sink rate and used power spectral density analysis to identify dominant frequencies in the yaw-rate data. As mentioned above, all data were sampled at 20 Hz and then divided into 2048-point blocks with 50% overlap. The sink rate, the variance of the yaw rate, and the tail-beat frequency were computed per each block and associated with central time of the block data. Power spectral density was calculated as the average of all relevant blocks.

Biomechanical model

We constructed a biomechanical model to estimate the energy savings of a shark in updraft zones. The mechanical power a shark needs to swim at speed v is $P_h = Dv/\eta_h$, where D is the hydrodynamic drag, and η_h is the hydrodynamic propulsion efficiency. When swimming at constant depth without updrafts, power is supplied by the muscles and is directly responsible for the majority of the routine metabolic rate. For a negatively buoyant shark, loss of potential energy during descent can supply a proportion of this power, $P_d = Wv_d$, where W is the submerged weight and v_d is the sink rate. The sink rate at which all the mechanical power needed for locomotion is provided by the loss of potential energy (i.e. when $P_d = P_h$) is

$$V_d = Dv/(\eta_h W). \quad (1)$$

At this sink rate the shark can swim at constant speed without any muscle activity. Swimming at constant depth in an updraft of velocity v_u will save the shark v_u/V_d of the locomotive power P_h. For a typical requiem shark that swims at the speed that minimizes the cost of transport (COT), P_h is 1 to 1.5 times the standard metabolic rate P_0 (Iosilevskii and Papastamatiou 2016, Papastamatiou et al. 2018a). Hence, the potential saving in an updraft is comparable with the standard metabolic

rate.

We have estimated V_d by two methods. One was based on a single shark that swam offshore into pelagic waters, and started yo-yo diving. For this shark we used a linear regression between the variance of the yaw rate and the vertical speed, to find the rate of descent at which the variance of the yaw rate (and hence the muscle power) approaches zero. We also estimated V_d using the drag model described in Iosilevskii and Papastamatiou (2016). Setting

$$D = W\left(\frac{\rho v^2 S}{2W} C_{D0} + K\frac{2W}{\rho S v^2}\right), \tag{2}$$

in (1), we could find

$$V_d = \frac{v}{\eta_h}\left(\frac{v^2}{u_0^2} C_{D0} + K\frac{u_0^2}{v^2}\right), \tag{3}$$

where ρ is the density of water, S is the reference (maximal transverse body section) area, C_{D0} and *K* are drag coefficients (parasite and induced, respectively) and

$$u_0^2 = 2W/\rho S = 2k_{\mathrm{pc}}\beta g l\,. \tag{4}$$

is a certain quantity having dimensions of speed. The factors involved in the definition of u_0^2 are the acceleration of gravity *g*, the fork length *l*, the sinking factor β, and the prismatic coefficient (ratio of body volume to the volume of the smallest cylinder enclosing the body) k_{pc}. The last two factors, as well as the drag coefficients and the propulsion efficiency were previously estimated in Iosilevskii and Papastamatiou (2016) for a morphologically comparable species, the blacktip shark (*Carcharhinus limbatus*).

Results

Acoustic telemetry

The movements of 38 sharks (Total Length (TL): 141.0 ± 9.9 cm (mean ± 1SD), 34 F: 4 M)

were tracked from April–June 2018. However, only 33 individuals provided enough detections and were kept for analysis. Sharks used restricted areas that did not differ in size between incoming (95 % Kernel Utilization Distributions (KUD), mean ± 1SE, 0.188 ± 0.033 km^2) and outgoing (0.199 ± 0.036 km^2) tides (Fig. 1A). However, sharks shifted the core areas of space use between the tides, with their 50 % KUD relocating south and outside of the narrow part of the channel during the outgoing tide (Fig. 1A, 2). During the incoming tides, sharks swam at slightly deeper depths (mean ± SE: incoming = 19.2 ± 0.05 m, n = 18155; outgoing = 17.6 ± 0.04 m, n = 30398, GLMM: df = 1, F = 773.4, $p < 0.0001$, Fig. 1B), but reduced their overall activity relative to outgoing tides (mean ± SE: incoming = 0.58 ± 0.01 $m.s^{-2}$, n = 72178; outgoing = 0.73 ± 0.01 $m.s^{-2}$, n = 121286, GLMM: df = 1, F = 8141.5, $p < 0.0001$, Fig. 1C). There was a significant increase in group dispersion, with inter-individual distance between tagged sharks increasing during the outgoing tide, (mean ± SE: incoming = 453.2 ± 4.2 m, n = 4985; outgoing = 590.1 ± 3.5 m, n = 6624, ANOVA: df = 1, F = 42.77, $p < 0.0001$, Fig. 1D).

During the incoming tide, updrafts are predicted to form along the northern region of the channel as tidal currents collide with the slope (Fig. 2a). Updrafts also form at the southern entrance of the channel at the drop-off. When the tides switch direction, outgoing currents switch the location of updraft zones to the smaller (and deeper) slope within the southern section of the channel (Fig. 3a). Overlaying the occupation density (time spent in different regions) of reef sharks over the bathymetry and current model, highlights that sharks are spending most of their time using the sloping regions where updrafts are likely to occur, particularly during incoming tides (Fig. 2b, 3b). Furthermore, during incoming tides sharks move closer to the channel floor within updraft regions (Fig. 2a) but during the outgoing tides move into shallow water to avoid downdraft regions that have now formed (Fig. 3a). Our randomizations showed that sharks were spending more time

within updraft zones than predicted for randomly moving animals, both during incoming (0.35 vs 0.10 proportion points inside updraft zone empirical vs random, $p<0.001$) and outgoing tides (0.25 vs 0.11 proportion inside updraft empirical vs random, $p<0.001$, Supplementary material B).

Group kinematics

Video taken by divers during incoming tides showed that sharks face into the current and perform shuttling behavior; once they reach a region at the front of the group (south section) they allow the current to transport them to the back (north section, Supplementary material C for video). Sharks swimming at the front (south) section of the group had an average apparent TBF of 0.7 Hz while those at the back (north) north section swam at 0.4 Hz, although there was also a difference between groups, likely representing different current velocities (two-way ANOVA, $F=84.56$, $p<0.001$ for position, $F=4.86$, $p<0.001$ for group ID, Fig. 4A, B). When individual sharks were tracked moving from the front to the back of the group, their TBF decreased from 0.63 ± 0.05 Hz at the front to 0.27 ± 0.05 Hz at the rear of the group (mean ± 1SE, $F=28.6$, $p<0.001$, Fig. 4B). Incidentally, the rear of the group (north region) is where the updrafts are expected to be the largest (Fig. 2A). It is acknowledged that our method of estimating TBF is based on correct identification of the tail position, which becomes problematic when the tail amplitude diminishes. As such, a missed period could underestimate the TBF by 50 %. However, our goal was to compare swimming effort between sharks at the rear or front of the group, and a decrease in apparent TBF would be associated with reduced swimming effort, regardless if it was caused by a decrease in amplitude. Due to safety reasons and poor water visibility, we could not perform dives during the outgoing tides, so could not compare between tidal stages.

Biologging

We deployed biologging sensors on seven sharks (TL 148.0 ± 8.9 cm, 3 M: 4F) for durations

of 2–24 h (Table 1). All tags released within the channel with the exception of shark #3 which popped off 20 miles offshore, three days later (Table 1). Data from four sharks (one individual only provided video) that spanned a tidal cycle show that those sharks swam into shallower water and increased ODBA during the outgoing tide (Fig. 5, Supplementary material D). Sharks swam at depths of 20–25 m while in the channel during the incoming tide but swam at depths of 10–15 m during the outgoing tide. Overall dynamic body acceleration (ODBA) increased during outgoing currents, suggesting an increase in activity (Fig. 5). Pseudo-heading (derived from magnetometer data) showed that during incoming tides sharks displayed frequent changes of direction in the north-south axis, although overall they faced south into the incoming current (Fig. 5). During the outgoing tides, sharks faced north into the current, but there were minimal changes in direction. We obtained 21 h of video from four sharks, which highlighted changes in group dynamics with tidal currents (for two individuals video spanned the full tidal cycle). During incoming tides, sharks were within polarized groups (Fig. 5i) where they frequently changed direction (switching position from front to back every 2.1 ± 0.16 minutes, Supplementary material E1 for video). During slack tide, group structure broke down and sharks were milling in a large group (Fig. 5ii). Finally, during outgoing tides, sharks could be seen swimming closer to the surface either by themselves or in small groups of 4–6 individuals (Fig. 5iii, Supplementary material E2). The videos also revealed that outgoing currents generated high levels of turbulence, with the camera equipped shark and other sharks in frame bouncing around vertically with minimal movement of their tail (Supplementary material E2 for video). Only one feeding attempt was observed on camera, during the incoming current, with all sharks in the group chasing needlefish on the surface. Note that depth changes measured by biologgers are considerably more pronounced than those estimates from telemetry (see above). However, telemetry is sampling depth at lower temporal resolution

with lower accuracy, and is averaging across many individuals over several months. Hence, biologging represents fine-scale changes at the individual level, while telemetry represents population-level changes.

One shark left the channel and swam into open-ocean providing a serendipitous comparison between swimming outside vs inside the channel. The shark that left the channel swam using characteristic yo-yo dives to depths of 130 m that were particularly pronounced during the last two hours of deployment (Fig. 6). The proportionality factor between the sink rate and the variance of the yaw-rate for this individual was -1.64, while the variance at zero sink rate was 0.33 rad^2/s^2. Remarkably, the correlation coefficient between these two parameters during the last two hours of deployment was -0.96 (-0.77 over the entire data set). Tail beat frequency varied between 0.6–0.8 Hz. For the remaining sharks that stayed in the channel, the variance of the yaw-rate was 0.1–0.2 rad^2/s^2 at zero sink rate, and there was no correlation between the sink rate and the variance of the yaw rate (correlation coefficient between -0.21 and -0.25). All three sharks showed two peaks in the power spectral density of the yaw rate, one at low frequencies (close to 0 Hz), and one around 0.7 Hz (Fig. 6). The low frequency peak could be associated with the turbulence of the outgoing tides and with shuttling during the incoming tide (from video, see above); the higher frequency peak is associated with the tailbeat.

Biomechanical model

We could estimate V_d directly from swimming segments from shark # 3 that swam offshore (Table 1). This shark exhibited a linear relationship $\langle \dot{\psi}^2 \rangle = -1.64 v_d + 0.33$ between the variance of the yaw-rate $\langle \dot{\psi}^2 \rangle$ and the rate of descent v_d (green and read data sets on Figs. 5a, b, c). As such, V_d could be estimated as the sink rate when $\langle \dot{\psi}^2 \rangle$ is zero, approximately at 0.2 m/s. Although we

did not measure swim speed, we can plausibly assume that it was at the speed that minimizes the COT, between 0.6 and 0.74 m/s (Papastamatiou et al. 2018a, see below).

We also determined V_d using equation (3) based on parameters previously estimated for a morphologically comparable species, the blacktip shark (*Carcharhinus limbatus*). Referring to Supplementary Table S1 in (Iosilevskii and Papastamatiou, 2016), C_{D0} ranges from 0.19 to 0.24; K between 0.03 and 0.05, and β and k_{pc} are estimated at 0.055 and 8/15, respectively. Assuming that the hydrodynamic propulsion efficiency η_h is between 0.7 and 0.8, we found that a 1.4 m grey reef shark should have V_d between 0.11 and 0.2 m/sec when swimming at 0.62 m/s (the lower estimate of its COT-optimal speed), and between 0.16 and 0.26 when swimming at 0.74 m/s (the upper estimate of its COT-optimal speed). Therefore, the estimate of 0.2 m/s for V_d is consistent with both methods. Based on this estimate, a 5 cm/s updraft would reduce locomotory costs by 25-35%. Assuming routine metabolic costs of requiem sharks are 2-2.5 x standard metabolic rate (Papastamatiou et al. 2018a), then reef sharks would reduce their routine metabolic rates by 10-15 % when in updrafts (see the paragraph immediately following equation (1)).

Discussion

Grey reef sharks use regions of the Fakarava channel where tidal currents collide with upward-facing slope areas and where updrafts are predicted to form. Sharks are negatively buoyant and updraft currents likely reduce the effort needed to stay at constant depth by counteracting the forces of gravity (Harris 1936, Lauder and Di Santo 2015, Iosilievskii and Papastamatiou 2016). By using these areas, sharks may conserve considerable energy, which likely contributes to the large numbers of sharks residing in the channel (Mourier et al. 2016). As such, we highlight the importance updrafts and the energy landscape may play in driving the distribution of negatively

buoyant marine predators.

Our first line of evidence is that sharks shift their core (50 % KUD) habitat use to locations which overlap with predicted updrafts areas. During incoming tides, these will form along the entrance of the channel and the slope within the northern region of the channel (also see Supplementary material A). During the outgoing tide, the predicted location of the updraft zone shifts south where there is a smaller slope facing the outgoing current, and sharks expand their core location south to include this region. However, during the outgoing tide the remainder of the channel is predicted to be in a downdraft. As the downdraft should decrease with increasing distance from the bottom (moving shallower), the shark's average swimming depth also decreases.

Secondly, our underwater observations and biologging show that during incoming tides, sharks face into the current but will shuttle so that they remain in the same overall region (Supplementary material B). While in predicted updraft zones (at the northern/rear region of the group), they swim with minimal effort and at times barely move their tails. The swimming effort markedly increases once they exit this region (now at the south/front region of the group) whereupon they let the current transport them back into the updraft zone. Telemetry also shows that during incoming tides, sharks are spending short amounts of time just south of the updraft zone, which corresponds with our underwater observations that individuals in the front/southern region of the group swim with greater effort.

Our third line of evidence was using high-resolution motion sensors (gyroscope) to estimate relative energy costs (Iosilevskii and Papastamatiou 2016). The shark swimming offshore displayed characteristic yo-yo diving, with reduced swimming activity during descents, behavior seen in many negatively buoyant sharks (Gleiss et al. 2011, Papastamatiou et al. 2018a). However, sharks in the channel demonstrated considerably reduced swimming effort to maintain depth, and

we predict that a 5 cm/sec updraft current will reduce the shark's routine metabolic rate by 10-15 %. Although we do not know the strength of updrafts, based on likely current speeds in the channel, this is a conservative estimate as a 5 cm/sec updraft can be associated with a relatively weak 0.25–0.5 m/s incoming current (see the warm-colored regions on Fig. 2 that mark updrafts in excess of 0.1 times the current speed). Similarly, birds fitted with inertial and altitude sensors showed reduced movement-induced energy expenditure when flying over topography predicted to induce orographic updrafts (Scacco et al. 2019).

Hence, grey reef sharks appear to reduce energy expenditure in much the same way that birds reduce their energy expenditure by using regions of updrafts and thermals (Weimerskirch et al. 2016, Williams et al. 2020). However, unlike birds which may use updrafts for efficient movement or foraging, grey reef sharks rarely forage during the day, suggesting that daytime habitat selection is likely linked to an energetic refuge as these animals never stop swimming (Papastamatiou et al. 2018b). Similarly, negatively buoyant squid are thought to 'surf the slope' by riding the updraft on sloping reefs so this mechanism may be a common component of the energy landscape of negatively buoyant animals (O'Dor et al. 2002). Of course there are likely additional, non-mutually exclusive reasons for sharks aggregating in the channel. For instance, foraging activity is remarkably high at night due to the abundance of coral reef fishes in the channel (Mourier et al. 2016, Labourgade et al. 2020). One shark with a biologger that recorded at night, showed more active behavior during incoming tides, but behaved similarly to the others during the outgoing tides (Supplementary material D). Grey reef sharks are known to form social groups and the formation of associations and subsequent social foraging likely also contributes to shark aggregations and the year round residency of at least some individuals (Mourier et al. 2016, Papastamatiou et al. 2020).

The energy seascape is highly dynamic as evident by the changes in behavior of sharks during the outgoing tides. In addition to expanding their space use to match the new predicted updraft zone (see above), counter to our hypothesis, sharks stopped shuttling behavior and increase their activity. Animal-borne camera footage reveals that sharks are encountering strong turbulence during outgoing tides, but there appears to be little active swimming. We therefore believe that increased activity is due to sharks moving around in turbulence, but not necessarily due to increased muscle activity. Captive studies have shown some fish (e.g. trout) are able to reduce energy expenditure in turbulence by slaloming between vortices (Liao 2007, Liao et al. 2003), and turbulence may subsidize flight costs of flying birds when updrafts are not available (Mallon et al. 2016). Large scale turbulent eddies may play an important role in the energy seascapes of fishes and future work should incorporate computational fluid dynamic modelling to accurately predict their location. We expect updrafts to be weaker during outgoing tides as the slope is located in a deeper portion of the channel (where currents are weaker), and in combination with turbulence may explain why sharks are distributed over a large area, in shallower water, with greater dispersion between sharks.

Unlike studies with birds, where inertial sensors can be combined with GPS loggers, we are not able to directly combine high-temporal resolution measures of shark activity with their accurate spatial location (Papastamatiou et al. 2018b). GPS will not work underwater and biologgers must be physically recovered, generally reducing measurements to only a few days. We also were not able to directly measure updrafts and must rely on flow simulations based on bottom topography. Studies with birds are also rarely able to directly measure updrafts, but a recent study showed that predicting updrafts based on mountain topography may be at least as accurate as previous dynamic models, in predicting updraft location (Scacco et al. 2019). Unlike winds, tidal currents are very

predictable which means we can accurately determine the temporal shifts in updraft location. Due to our study taking place within a small, relatively confined location, and sharks being residential, we had the unique opportunity to match up shark movements and behavior with the likely location of updrafts. It is unlikely that other abiotic factors could explain habitat shifts with tides (e.g. temperature or oxygen levels) as core use shifts are only over spatial scales of 200 m.

While energy landscapes traditionally explain the extent of an animal's foraging range and movement paths (Wilson et al. 2012, Shepard et al. 2013), here we show that they may also explain aggregations of 'refuging' large marine predators. Our combination of methods reveals how important the energy seascape may be for understanding the distribution and habitat selection of marine predators, despite this approach rarely being considered for fishes (Sheppard et al. 2013). It also highlights how aggregations and large groups of animals may form in locations where all individuals reduce energy expenditure. Marine predators such as sharks are well known to aggregate within hotspots but the drivers of these patterns have not been quantified (Hearn et al. 2010, Hays et al. 2016, Desbiens et al. 2021). While we only identify how the energy seascape may influence shark distribution over small spatial scales, the implications of energy seascapes may be much larger (e.g. Somerville et al. 2018). For example, a recent study found that shark abundance throughout the northern Great Barrier Reef was positively correlated with current strength, potentially through the actions of updrafts (Desbiens et al. 2021). Anthropogenic modification of habitats may also alter updraft locations and intensity, which will change energy landscapes (e.g. birds and windfarms, Péron et al. 2017). There is therefore, the potential for anthropogenic modification of coastal environments to alter the distribution and behavior of marine animals that use updraft zones.

Acknowledgements: This study was conducted at the request and under the authority of the Direction de environment de Polynésie française (DIREN) under the convention 4469/MCE/ENV signed on 11 June 2017. Funding was provided by Blancpain Ocean Commitment. Sponsors supporting the expedition include: Tahiti Tourisme, Air Tahiti Nui, Aqualung, Nikon, Seacam, Aqualung and ApDiving. We would like to thank C. Gentil, Y. Gentil, T. Rauby, C. Ballesta, and many others of the Gombessa Expedition to Fakarava, for assistance in the field. We also thank S. A. Richemond and the Tetamanu lodging staff for hosting us in Fakarava. We thank S. Luongo for analysis of biologging data. Shark tagging was approved by FIU IACUC #200787. The authors confirm that there are no conflicts of interest with this work. This is contribution # 269 from the Coastlines and Oceans Division of the Institute of Environment at Florida International University.

Author Contribution: YPP, CH, JM, and SP conceived the study. GI performed all biomechanical modelling. GI, VDS, TH, YPP, CH and JM analyzed data. YPP, CH, LB and JM performed fieldwork. YPP wrote the paper with input from all authors.

Data availability: Acoustic telemetry data can be found in Dryad Dataset, Papastamatiou et al. 2021

References:

Amėlineau, F., Pėron, C., Lescroël, A., Authier, M., Provost, P., Grėmillet, D. (2014). Windscape and tortuosity shape the flight costs of gannets. *Journal of Experimental Biology* 217, 876-885

Amėlineau, F, Fort, J., Mathewson, P.D., Speirs, D.C., Courbin, N., Perret, S., Porter, W.P., Wilson, R.J., Grémillet, D. (2018). Energyscapes and prey fields shape a North Atlantic seabird wintering hotspot under climate change. *Royal Society Open Science* 5, 171883

Bidder, O.R., Walker, J.S., Jones, M.W., Holton, M.D., Urge, P., Scantlebury, D.M., Marks, N.J.,

Magowan, E.A., Maguire, I.E., Wilson, R.P. (2015). Step by step: reconstruction of terrestrial animal movement paths by dead reckoning. *Movement Ecology* 3:23

Brill, R.W., Holts, D.B., Chang, R.K.C., Sullivan, S., Dewar, H., Carey, F.G. (1993). Vertical and horizontal movements of striped marlin (*Tetrapturus audax*) near the Hawaiian Islands, determined by ultrasonic telemetry, with simultaneous measurements of oceanic currents. *Marine Biology* 117, 567-574

Desbiens, A.A., Roff, G., Robbins, W.D., Taylor, B.M., Castro-Sanguino, C., Dempsey, A., Mumby, P.J. (2021). Revisiting the paradigm of shark-driven cascades in coral reef ecosystems. *Ecology* In Press.

Duerr, A.E., Miller, T.A., Dunn, L., Bell, D.A., Bloom, P.H., Fisher, R.N., Tracey, J.A., Katzner, T.E. (2019). Topographic drivers of flight altitude over large spatial and temporal scales. *Auk* 136, 1-11

Di Santo, V., Kenaley, C.P., Lauder, G.V. (2017). High postural costs and anaerobic metabolism during swimming support the hypothesis of a U-shaped metabolism-speed curve in fishes. *Proceedings of the National Academy of Sciences* 114, 13048–13053

Dunford, C.E., Marks, N.J., Wilmers, C.C., Bryce, C.M., Nickel, B., Wolfe, L.L., Scantlebury, D.M., Williams, T.A. (2020). Surviving in steep terrain: a lab-to-field assessment of locomotor costs for wild mountain lions (*Puma concolor*). *Movement Ecology* 8, 34

Furness, R.W., Bryant, D.M. (1996). Effect of wind on field metabolic rates of Northern Fulmars. *Ecology* 77, 1181-1188

Gleiss, A.C., Norman, B., Wilson, R.P. (2011). Moved by that sinking feeling: variable diving geometry underlies movement strategies in whale sharks. *Functional Ecology* 25, 595-607

Harris, J.E. (1936). The role of the fins in the equilibrium of the swimming fish. I. Wind-tunnel

tests on a model of *Mustelus canis*. *Journal of Experimental Biology* 13, 476-493

Hays, G.C. et al. (2016). Key questions in marine megafauna movement ecology. *Trends in Ecology and Evolution* 31, 464-475

Hearn, A., Ketchum, J., Klimley, A.P., Espinoza, E., Penaherrera, C. (2010). Hotspots within hotspots? Hammerhead shark movements around Wolf Island, Galapagos Marine Reserve. *Marine Biology* 157, 1899-1915

Iosilevskii, G., Papastamatiou, Y.P. **(**2016). Relations between morphology, buoyancy and energetics of requiem sharks. *Royal Society Open Science* 3, 160406

Katz, K., Plotkin, J. (1991). Low speed aerodynamics. McGraw Hill, New York. Pp 303-313

Labourgade, P., Ballesta, L., Huveneers, C., Papastamatiou, Y.P., Mourier, J. (2020). Heterospecific foraging associations between reef-associated sharks: first evidence of kleptoparasitism in sharks. *Ecology* 101, e03117

Lauder, G.V., Di Santo, V. (2015). Swimming mechanics and energetics of elasmobranch fishes. In: *Fish Physiology* (eds RE Shadwick, AP Farrell, CJ Brauner). Cambridge, Academic Press. pp. 219– 253

Liao, J.C., Beal, D.N., Lauder, G.V., Triantafyllou, M.S. (2003). Fish exploiting vortices decrease muscle activity. *Science* 302, 1566-1569

Liao, J.C. (2007). A review of fish swimming mechanics and behavior in altered flows. *Philosophical Transactions of the Royal Society B* 362, 1973-1993

Mallon, J.M., Bildstein, K.L., Ktazner, T.E. (2016). In-flight turbulence benefits soaring birds. *Auk* 133, 79-85

Marigliano, D., Taquet, M. (2011). Étude des courants de la passe ‘Kaki’ de l’atoll de Hao. Évaluation du gisement hydrolien, Issy, Ifremer, coll. Ressources Biologiques et

Environnement. Disponible en ligne sur: wwz. ifremer. fr/cop/content/download/51828/735995/file/Rapport% 20Ifremer% 20Etude% 20des% 20courants.

McElroy, B., DeLonay, A., Jacobson, R. (2012). Optimum swimming pathways of fish spawning migrations in rivers. *Ecology* 93, 29-34

McInturf, A.G., Steel, A.E., Buckhorn, M., Sandstrom, P., Slager, C.J., Fangue, N.A., Klimley, A.P., Caillaud, D. (2019). Use of a hydrodynamic model to examine behavioral response of broadnose sevengill sharks (*Notorynchus cepedianus*) to estuarine tidal flow. *Environmental Biology of Fish*es 102, 1149-1159

Mourier, J., Maynard, J., Parravicini, V., Ballesta, L., Clua, E., Domeier, M.L., Planes, S. (2016). Extreme inverted trophic pyramid of reef sharks supported by spawning groupers. *Current Biology* 26, 2011-2016

O'Dor, R.K., Adamo, S., Aitken, J.P., Andrade, Y., Finn, J., Hanlon, R.T., Jackson, G.D. (2002). Currents as environmental constraints on the behavior, energetics and distribution of squid and cuttlefish. *Bulletin of Marine Science* 71, 601-617

Papastamatiou, Y.P.**,** Iosilevskii, G., Leos-Barajas, V., Brooks, E.J., Howey, L.A., Chapman, D.D., Watanabe, Y.Y. (2018a). Optimal swimming strategies and behavioural plasticity of oceanic whitetip sharks. *Scientific Reports* 8, 551

Papastamatiou, Y.P., Watanabe, Y.Y., Demšar, U., Leos-Barajas, V., Bradley, D., Langrock, R., Weng, K., Lowe, C.G., Friedlander, A.M., Caselle, J.E. (2018b). Activity seascapes highlight central place foraging strategies in marine predators that never stop swimming. *Movement Ecology* 6, 9

Papastamatiou, Y.P., Bodey, T.W., Caselle, J.E., Bradley, D., Freeman, R., Friedlander, A.M., Jacoby, D.M.P. (2020). Multiyear social stability and social information use in reef sharks

with diel fission-fusion dynamics. *Proceedings of the Royal Society B*. 287, 20201063

Papastamatiou, Y.P. et al. (2021). Sharks surf the slope: current updrafts reduce energy expenditure for aggregating marine predators. Dryad Dataset https://doi.org/10.5061/dryad.00000003q

Péron, G., Fleming, C.H., Duriez, O., Fluhr, J., Itty, C., Lambertucci, S., Safi, K., Shepard, E.L.C., Calabrese, J.M. (2017). The energy landscape predicts flight height and wind turbine collision hazard in three species of large soaring raptor. *Journal of Applied Ecology* 54, 1895-1906

Rougerie, F., Gros, R. (1980). Les courants dans la passe d'Avatoru: atoll de Rangiroa, archipel des Tuamotu. Notes et documents d'oceanographie. N°1980/17. 30pp.

Scacco, M., Flack, A., Duriez, O., Wikelski, M., Safi, K. (2019). Static landscape features predict uplift locations for soaring birds across Europe. *Royal Society Open Science* 5, 181440

Shepard, E.L.C., Wilson, R.P., Rees, W.G., Grundy, E., Lambertucci, S.A., Vosper, S.B. (2013). Energy landscapes shape animal movement ecology. *American Naturalist* 182, 298-312

Simpfendorfer, C.A., Heupel, M.R., Hueter, R.E. (2002). Estimation of short-term centers of activity from an array of omnidirectional hydrophones and its use to study animal movement. *Canadian Journal of Fisheries and Aquatic Sciences* 59, 23-32

Somveille, M., Rodrigues, A.S.L., Manica, A. (2018). Energy efficiency drives the global seasonal distribution of birds. *Nature Ecology and Evolution* 2, 962-969

Taguchi, M., Liao, J.C. (2011). Rainbow trout consume less oxygen in turbulence: the energetics of swimming behaviors at different speeds. *Journal of Experimental Biology* 214, 1428-1436

Wall, J., Douglas-Hamilton, I., Vollrath, F. (2006). Elephants avoid costly mountaineering. *Current Biology* 16, R527-R529

Weimerskirch, H., Bishop, C., Jeanniard-du-Dot, T., Prudor, A., Sachs, G. (2016). Frigate birds track atmospheric conditions over months-long transoceanic flights. *Science* 353, 74-78

Wheeler, S., Robbins, W.D., McIllwain, J., Robbins, W.D. (2013). Reef sharks clean up with a novel inshore mutualistic interaction. *Coral Reefs* 32, 1089

Williams, H.J., Shepard, E.L.C., Holton, M.D., Alarcon, P.A.E, Wilson, R.P., Lambertucci, S.A. (2020). Physical limits of flight performance in the heaviest soaring bird. *Proceedings of the National Academy of Sci*ence 117, 17884-17890

Williamson, M.J., Dudgeon, C., Slade, R. (2018). Tonic immobility in the zebra shark, *Stegostoma fasciatum*, and its use for capture methodology. *Environmental Biology of Fishes* 101, 741-748

Wilson, R.P., Culik, B., Adelung, D., Coria, N.R., Spairani, H.J. (1991). To slide or stride: when should Adélie penguins (*Pygoscelis adeliae*) toboggan? *Canadian Journal of Zoology* 69, 221-225

Wilson, R.P., Quintana, F., Hobson, V.J. (2012). Construction of energy landscapes can clarify the movement and distribution of foraging animals. *Proceedings of the Royal Society B* 279, 975-980

Yates, G.T (1983). Hydromechanics of body and caudal fin propulsion. In *Fish Biomechanics* (Weihs D. and Webb PW eds.). New York, Praeger. Pg:177-213

Table 1. Sharks tagged with biologging sensors including a CATS diary (depth/temperature/3D acceleration/magnetometer/gyroscope) and video camera. * indicates individuals where only diary data was obtained while ** indicates only video was obtained.

Shark	Date	Total length (cm)	Sex	Duration (h)
1*	6/20/17	149	M	2
2*	6/27/17	146	F	10
3*	6/29/17	155	M	9
4	10/28/17	154	M	6
5	5/24/18	142	F	6
6	5/28/18	132	F	7
7**	5/29/18	158	F	24

Figure 1. Change in grey reef shark space use and behavior based on tidal stage. (A) Changes in space use (kernel utilization distributions) during incoming and outgoing tides by 33 acoustically tagged grey reef sharks. Circles represent the location of acoustic receivers. B) Corresponding changes in shark swimming depth, C) activity (body acceleration) and D) inter-shark distances (of tagged sharks only) during incoming (green) and outgoing (orange) tides.

Figure 2. Predicted location of updrafts and shark habitat use during incoming tides. Colour contours are the predicted ratio of vertical and tidal velocities (a). Circles represent average swimming depths of sharks from telemetry data. (b) Occupational density representing proportion of time sharks spend in different regions of the channel (see Fig. 1).

Figure 3. Predicted location of updrafts and shark space use during outgoing tides. Colour contours are the predicted ratio of vertical and tidal velocities (a). Circles represent average swimming depths of sharks from telemetry data. (b) Occupational density representing proportion of time sharks spend in different regions of the channel.

Figure 4. Grey reef shark apparent tail beat frequencies (TBF) as a function of position in the group (front (south) or back (north)) determined from diver video. A) Front vs back comparisons. B) Change in apparent TBF for individual sharks shuttling between front and back group positions. All video were taken during incoming tides.

Figure 5. Biologging data from grey reef sharks #5 (A) and #6 (B) during switching tides. The shaded area represents the outgoing tide. Sensors include swimming depth (dark red), Overall Dynamic Body Acceleration (ODBA, black) and magnetic heading (blue). Pseudo-heading values switching between 0 and 5 signify changes in direction along the South-North axis. Animal-borne video images from shark #6 show polarized swimming in tight groups during incoming tides (i), shoaling during slack tide (ii) and greater dispersion of the group in turbulent outgoing tides (iii).

Figure. 6. Swimming parameters of sharks within and outside the Fakarava channel. Data is for sharks #3 (a-c), #6 (d-f), #2 (g-i), and #5 (j-l). Shark #3 (top row) swam into open-ocean while all other individuals remained within the channel. First column is the relationship between sinking rate and the variance of the yaw angular rate (from gyroscope). The second column shows dominant frequencies in the angular rate (from power spectral density (PSD) analysis). The third column is the corresponding changes in depth. Every point on the left and right columns represents a 2048-points data-set (sampled at 20 Hz), with 1024 points overlapping with

the preceding set. PSD is an average of all relevant data sets. Black is for all data, blue is for either the first or last 2 hours of data, red represents ascents, green is descents. In Column 3, blue-colored subset roughly corresponds to the strongest incoming tide. ‘H’ and ‘L’ letters correspond to high and low tide respectively.

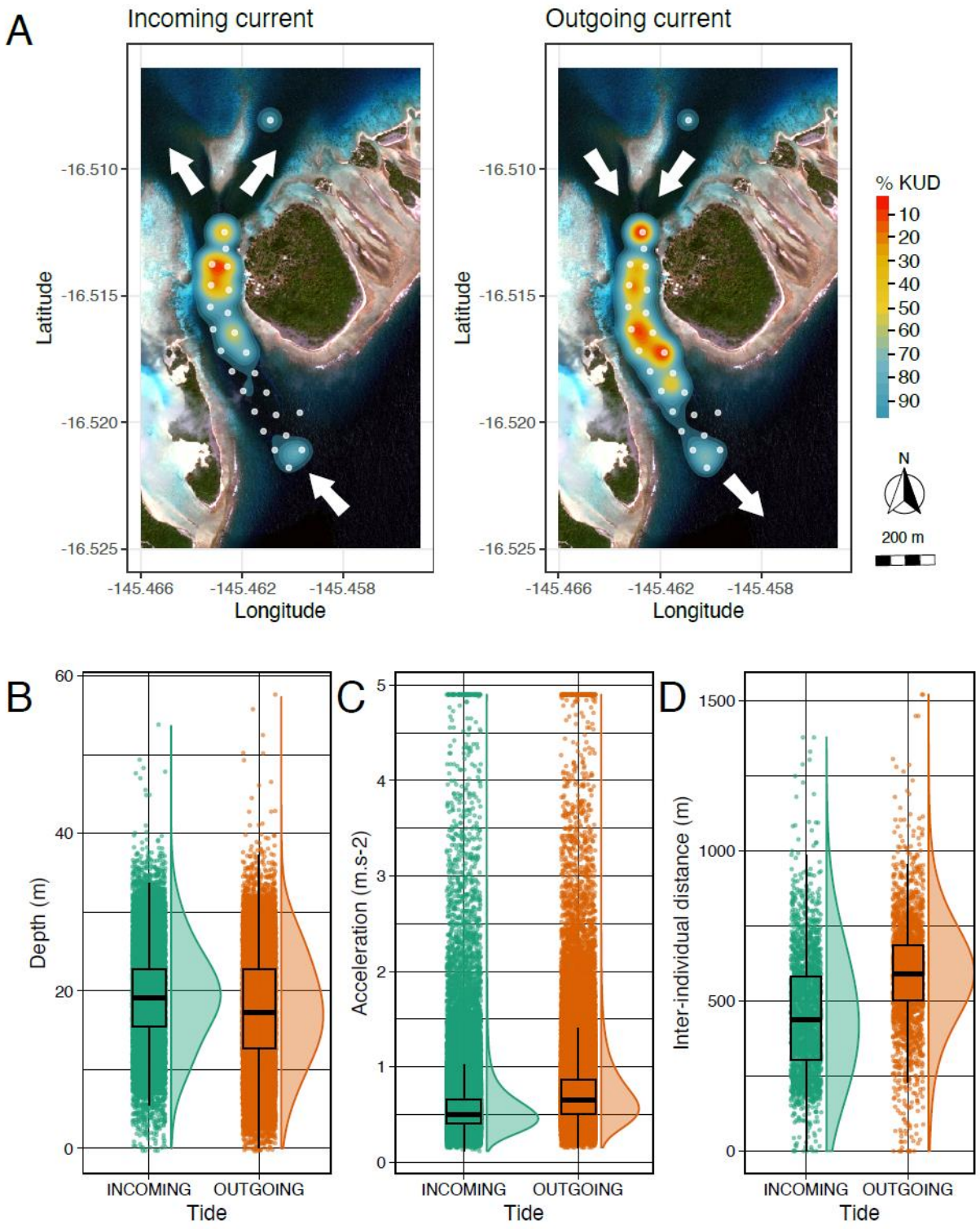
A
Incoming current
Outgoing current
Latitude
Longitude
-16.510
-16.515
-16.520
-16.525
-145.466
-145.462
-145.458
% KUD
10
20
30
40
50
60
70
80
90
N
200 m
B
Depth (m)
C
Acceleration (m.s-2)
D
Inter-individual distance (m)
INCOMING
OUTGOING
Tide

Fig. 1

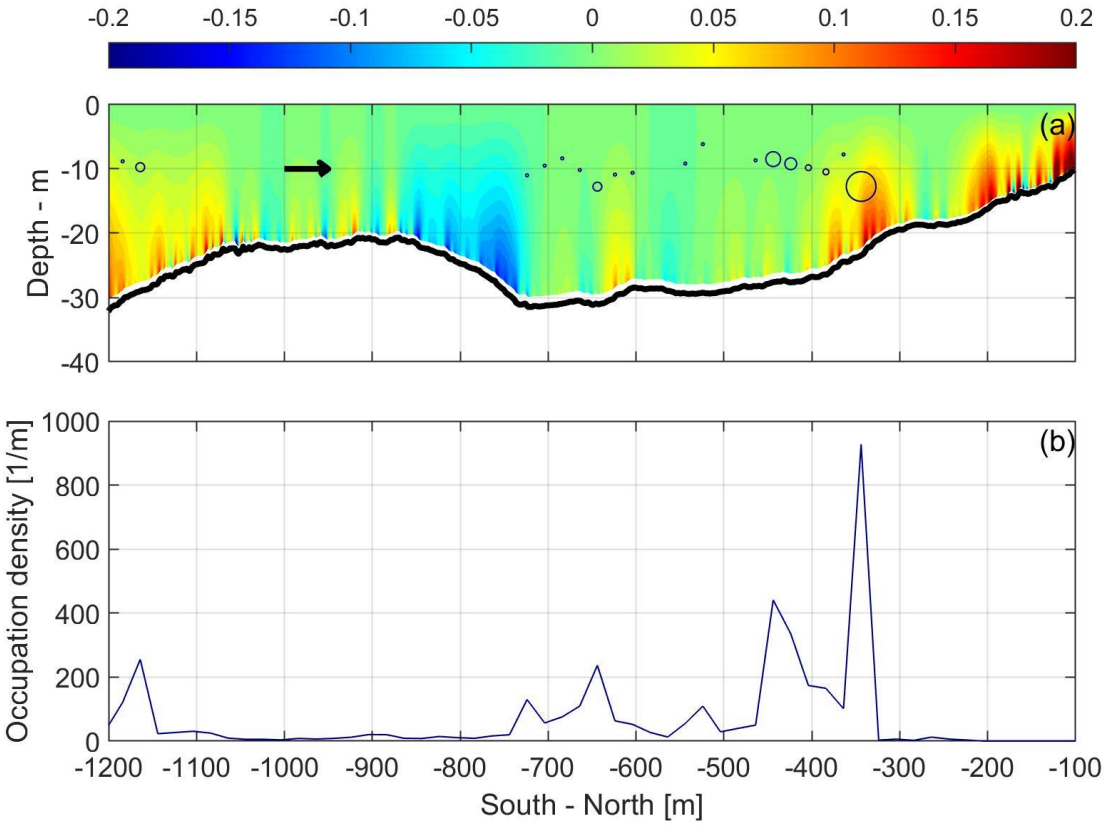
-0.2
-0.15
-0.1
-0.05
0
0.05
0.1
0.15
0.2
Depth - m
0
-10
-20
-30
-40
(a)
Occupation density [1/m]
1000
800
600
400
200
0
(b)
-1200
-1100
-1000
-900
-800
-700
-600
-500
-400
-300
-200
-100
South - North [m]

Fig. 2

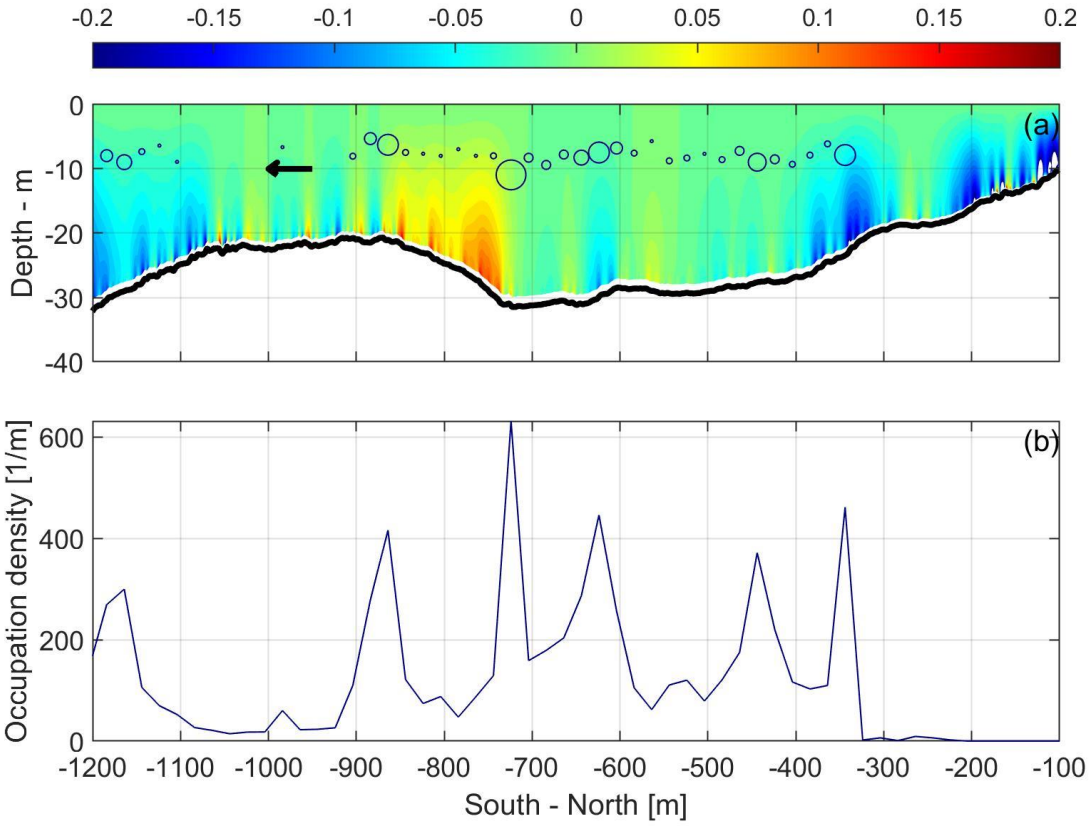
-0.2
-0.15
-0.1
-0.05
0
0.05
0.1
0.15
0.2
Depth - m
0
-10
-20
-30
-40
(a)
Occupation density [1/m]
600
400
200
0
(b)
-1200
-1100
-1000
-900
-800
-700
-600
-500
-400
-300
-200
-100
South - North [m]

Fig. 3

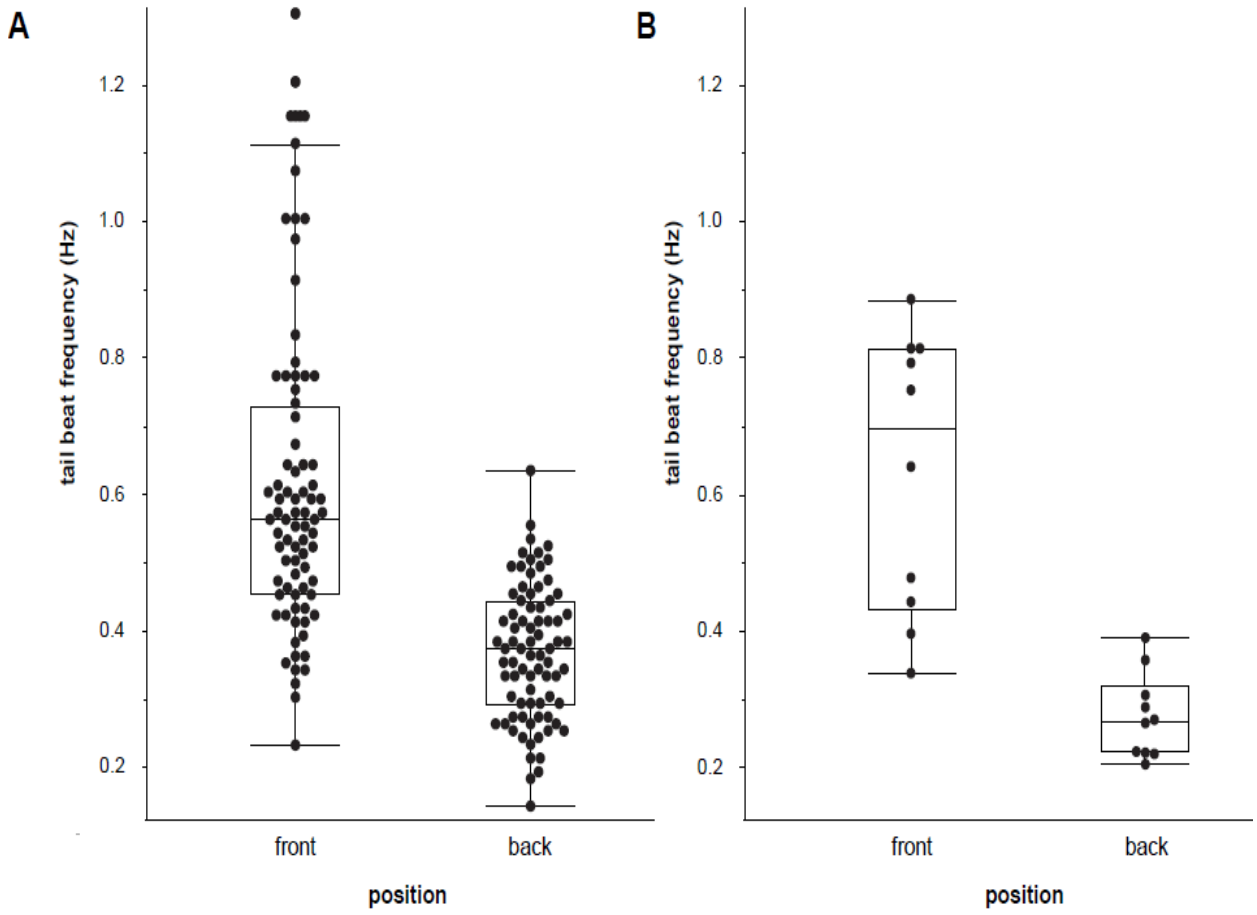
A
B
tail beat frequency (Hz)
1.2
1.0
0.8
0.6
0.4
0.2
front
back
position

Fig. 4

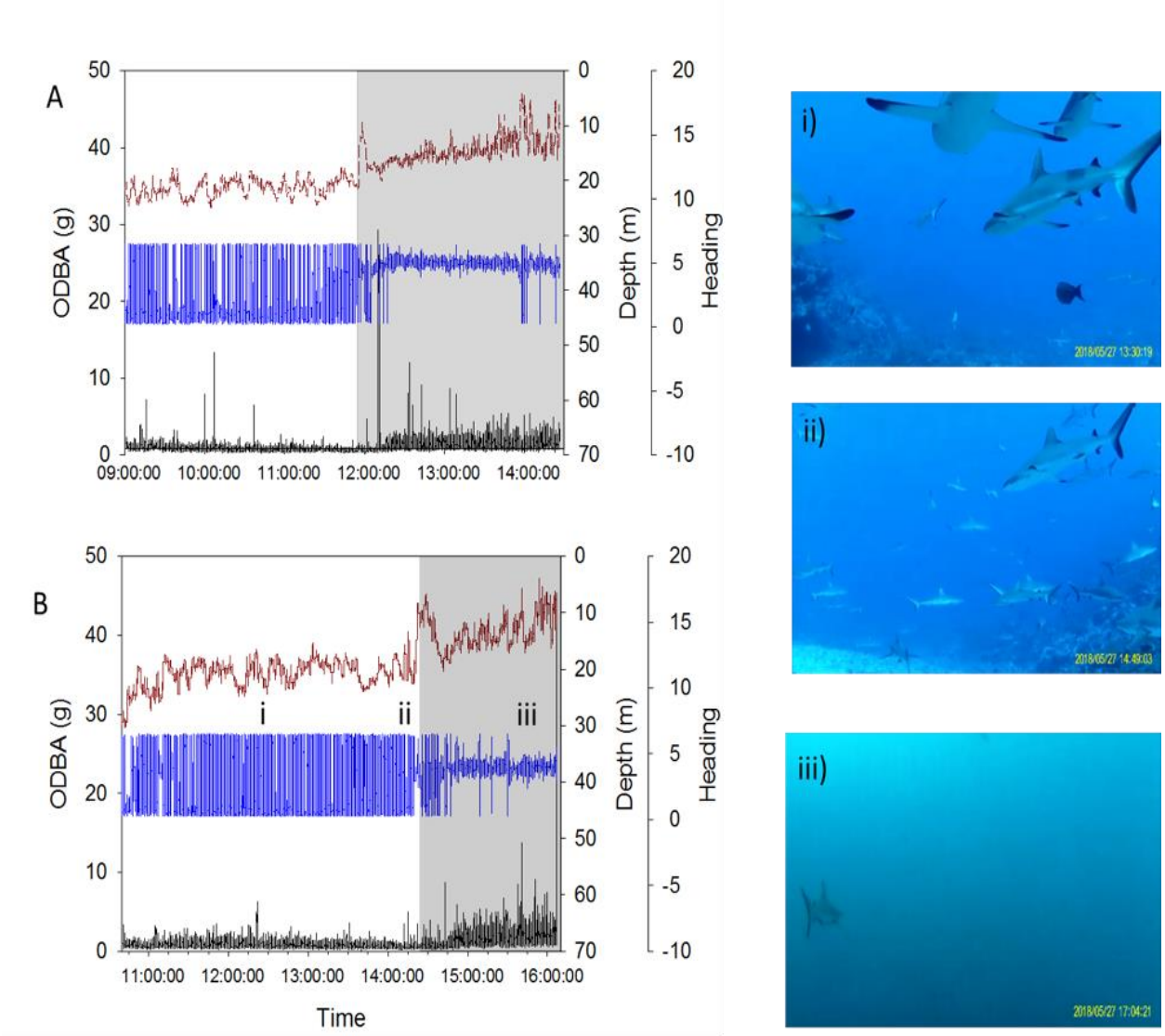
A
B
ODBA (g)
Depth (m)
Heading
09:00:00
10:00:00
11:00:00
12:00:00
13:00:00
14:00:00
15:00:00
16:00:00
Time
i
ii
iii
i)
ii)
iii)
2018/05/27 13:30:19
2018/05/27 14:49:03
2018/05/27 17:04:21

Fig. 5

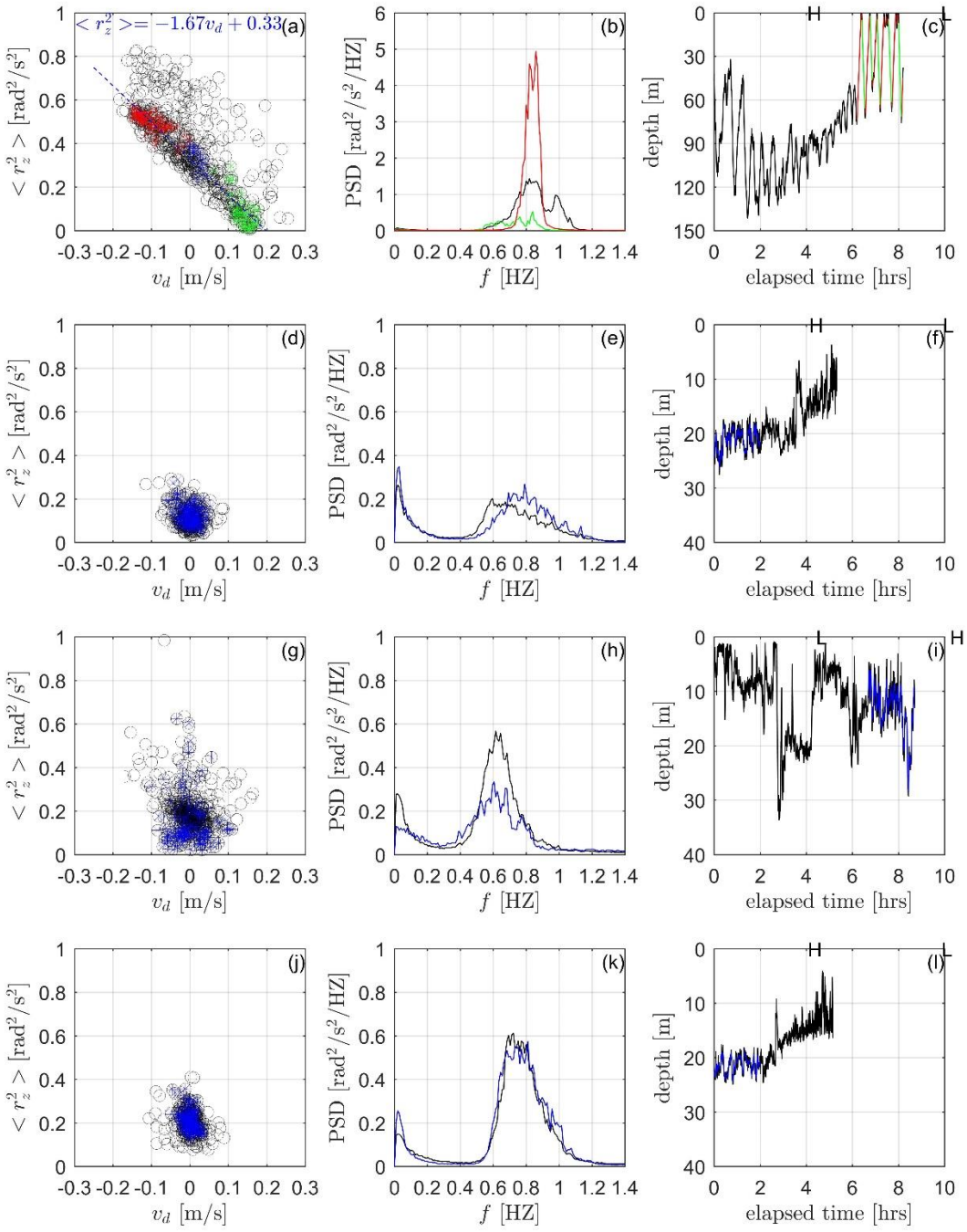
(a)
$< r_z^2 >= -1.67 v_d + 0.33$
$< r_z^2 >$ [rad^2/s^2]
v_d [m/s]
(b)
PSD [rad^2/s^2/HZ]
f [HZ]
(c)
H
L
depth [m]
elapsed time [hrs]
(d)
(e)
(f)
(g)
(h)
(i)
(j)
(k)
(l)

Figure 6

Supplementary Material

A) Location of shark groups within the Fakarava channel based on diver surveys and bathymetry of the channel.

B) Kernel Utilization Distributions of grey reef sharks in the Fakarava channel (orange/green contours) compared to predicted space use from randomizations (white dashed lines). Empirical space use is compared to random for both incoming and outgoing tides.

C) Diver video of grey reef shark shuttling behavior in the channel. Note sharks are facing into the incoming tidal current.

D) Changes in activity (ODBA, black), heading (blue), and swimming depth (red) for grey reef shark #2 during the night time period. Note the increase in activity and reduction in direction change during outgoing tides at approximately 6 am.

E) Animal borne-video footage showing change in behavior and grouping during incoming (D1), and outgoing tides (D2).

Supplementary material A

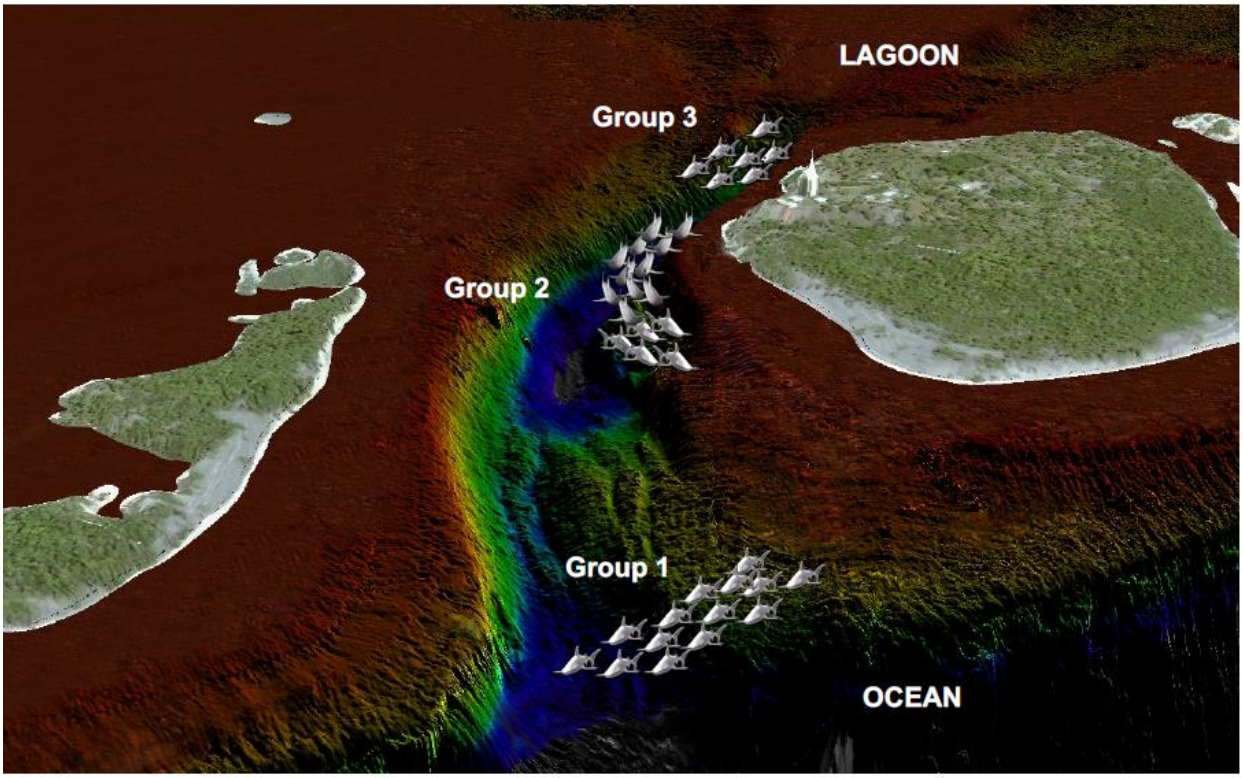

Supplementary material B

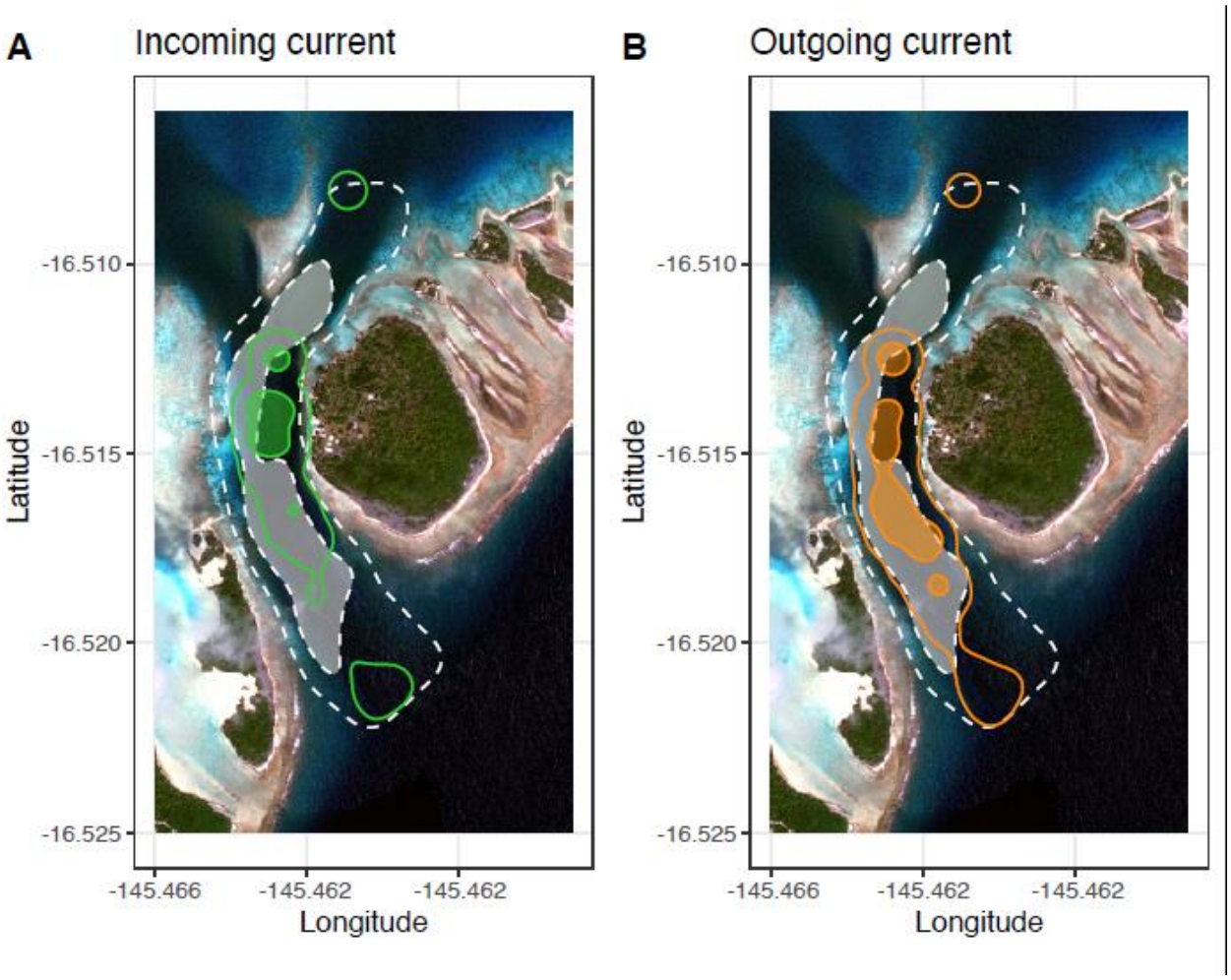

Supplementary material D